Search for Br* production in the D+DBr reaction

Jianyang Zhang,[a] Justin Jankunas, Nate C.-M. Bartlett, Noah T. Goldberg,[b] and Richard N. Zare[c]
Department of Chemistry, Stanford University, Stanford, California 94305-5080, USA

(Received 21 September 2009; accepted 26 January 2010; published online 22 February 2010)

Deuterium bromide (DBr) is expanded from a pulsed jet into a vacuum and a synchronized pulsed laser causes photodissociation of some of the DBr molecules to produce primarily (~85%) ground-state bromine atoms ($^2P_{3/2}$) and fast D atoms. The latter collide with the cold DBr molecules and react to produce molecular deuterium (D_2) via two possible channels, the adiabatic channel $D_2+Br(^2P_{3/2})$ and the nonadiabatic channel $D_2+Br^*(^2P_{1/2})$, which are asymptotically separated in energy by the spin-orbit splitting (0.457 eV) of the bromine atom. Ion images are recorded for $D_2(v'=1,\ J'=16,\ 18-21)$, $D_2(v'=2,\ J'=6,7,\ 10-12,\ 14-16)$, and $D_2(v'=3,\ J'=2-5)$ for various collision energies. For the nonadiabatic production of spin-orbit-excited Br* in the D+DBr reaction for the conditions studied we estimate that this channel contributes 1% or less. © *2010 American Institute of Physics*. [doi:10.1063/1.3319717]

I. INTRODUCTION

The $H+HX\rightarrow H_2+X$ reaction and its reverse reaction $X+H_2\rightarrow HX+H$, where X is a halogen atom, has been a topic of much interest. Spin-orbit interaction causes the lowest electronic state of the halogen atom to be split into two levels, the $^2P_{3/2}$ level as the ground state, denoted simply as X, and the first excited state, $^2P_{1/2}$, which is denoted by X*. The spin-orbit splitting ranges from 0.0038 eV for F, 0.198 eV for Cl, 0.457 eV for Br, to 0.935 eV for I. A controversial question is what role does X* play in the H+HX or $X+H_2$ reactions.

The $F+H_2$ reaction is famous for its vibrational population inversion.[1] Lee and co-workers using crossed molecular beams found no evidence for an F* contribution to this reaction. More recently, Nesbitt and co-workers[2] studied the single collision reactive scattering dynamics of $F+HD\rightarrow HF(v',J')+D$ using high-resolution infrared laser absorption for quantum state resolved detection of the nascent $HF(v',J')$ product states. They found several rotational states in the $HF(v'=3)$ vibrational manifold that are energetically inaccessible to the $F(^2P_{3/2})$ reagent. These arise from reactions with spin-orbit-excited $F^*(^2P_{1/2})$ but this nonadiabatic channel represents a minor ($\leq$5%) contribution to the reaction rate. Subsequently, Yang and co-workers[3] using Rydberg tagging found that $F^*(^2P_{1/2})$ is ~1.6 times more reactive than $F(^2P_{3/2})$ with D_2 at a collision energy (0.011 eV) for F that is only slightly below the barrier to reaction, but as the collision energy increases, the adiabatic channel rapidly dominates.

For $Cl+H_2$, Liu and co-workers[4,5] reported that $Cl^*(^2P_{1/2})$ is more reactive than $Cl(^2P_{3/2})$ in crossed-beam studies. Moreover, they found that the nonadiabatic channel increases in importance as the collision energy is increased. Many additional experimental studies have been carried out for this reaction system,[6–8] but in sharp contrast only a very small nonadiabatic contribution has been reported.

Leone and Nesbitt[9] examined inelastic and reactive scattering of $Br^*(^2P_{1/2})$ with H_2 under thermal conditions. They photolyze Br_2 to create hot Br and Br* atoms, but these become thermalized by collisions with excess argon. Admittedly, for collisions with $H_2(v=0)$ there is insufficient energy for reaction but for $H_2(v=1)$ they report that a significant fraction of the $Br^*+H_2(v=1)$ collisions proceed with direct reaction. This result is quite intriguing because microscopic reversibility ideas would imply efficient $Br^*+H_2(v=1)$ formation from the reverse H+HBr reaction, provided that these collisions could sample a similar distribution of $HBr(v,J)$ internal states and H+HBr center of mass kinetic energies. To date, the only previous experimental studies[10–12]of H+HBr were unable to answer whether or not Br* is formed. Consequently, we decided to reexamine the $H+HBr(v=0)$ reaction using ion imaging, which would allow us to observe directly if Br* is formed in this reaction. For reasons involving increased signal-to-noise ratio, we chose to study $D+DBr(v=0)$ and detect the speed distribution of the resulting D_2 product. This choice avoids the H_2 background of our instrument, seems to produce less dimerization, and makes this study possible in the present apparatus.

In what follows, we present information on how the experiment was done. We then describe the results that we have found, which imply at most, a very minor contribution of the nonadiabatic channel to the reaction under the conditions we studied.

II. EXPERIMENTAL

The apparatus used for this experiment has been described previously in detail.[13,14] A mixture of 3%–6% DBr in

[a]Present address: Dalian Institute of Chemical Physics, Dalian, China 116023.
[b]Present address: Agilent Technologies, 5301 Stevens Creek Blvd, Santa Clara, CA 95051 USA.
[c]Author to whom correspondence should be addressed. Electronic mail: zare@stanford.edu.

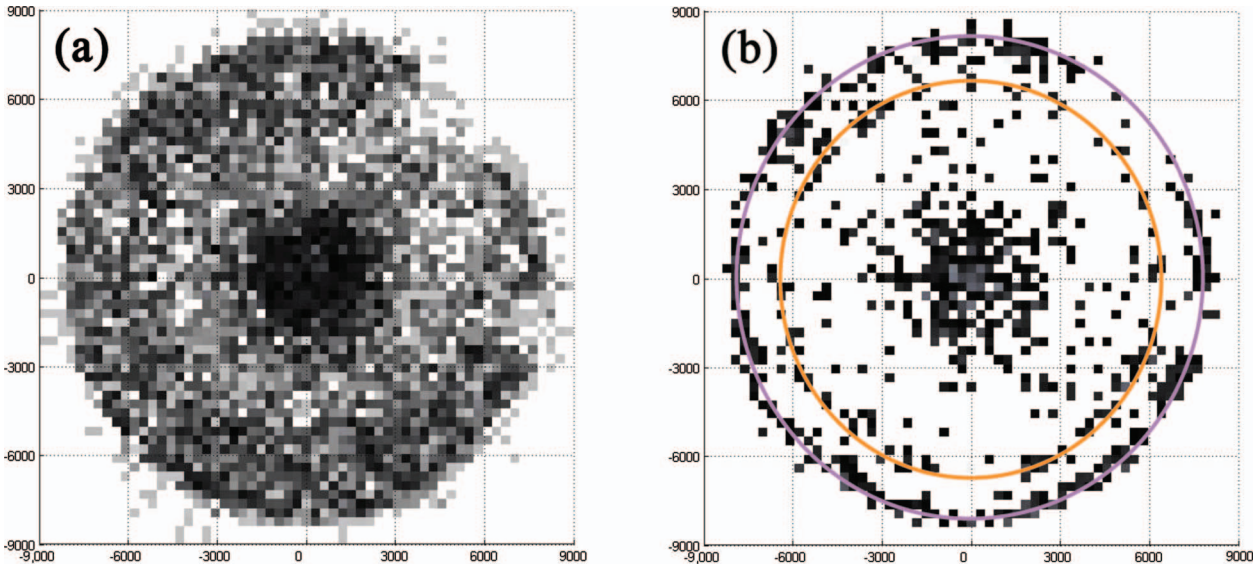

FIG. 1. Typical raw data for the detection of D_2 ($v'=2$, $J'=11$), showing (a) the three-dimensional crushed ion image and (b) the corresponding center slice. Two rings are clearly seen in the sliced image. The outer ring (purple circle to guide the eyes) corresponds to products from channel (1a) and the inner ring (orange circle) to those from channel (1c).

H_2 was supersonically expanded through a pulsed nozzle (General Valve Series 9) operating at 10 Hz with a backing pressure of ~1000 Torr and entered the extraction region of a Wiley–McLaren time-of-flight (TOF) mass spectrometer. The molecular beam is subsequently intersected at right angles by two linearly polarized and counterpropagating, focused UV laser pulses. The first of the two laser pulses cleaves the DBr bond, producing fast D atoms with a well defined speed and spatial anisotropy, which determines the center-of-mass collision energy for the system. It should be noted that photolysis of DBr proceeds via two channels, one that produces ground-state $Br(^2P_{3/2})$ atoms, the other that produces spin-orbit-excited $Br(^2P_{1/2})$ atoms, which is referred to as Br^*.[13] Over this wavelength range, the branching ratio for these two channels is nearly constant with $Br^*/Br \approx 0.18$.[13] Thus, we obtain D atoms from the DBr photolysis with two different speed distributions which we refer to as fast and slow D atoms. The wavelength range used for the photolysis pulse was 207–225 nm, which corresponds to a collision energy range of 1.43–2.11 eV for the fast D-atom channel. The difference in energy from the spin-orbit interaction is 0.457 eV, which corresponds to a difference in center-of-mass collision energies of 0.43 eV for the fast and slow D atoms. Therefore, the collision energy range for the slow D-atom channel is 1.00–1.68 eV.

After approximately 10 ns to allow for product build-up from single collisions with D atoms and unphotolyzed DBr and to be sufficiently short to prevent product fly-out, a second laser pulse with a slightly smaller focal volume (approximately 80% that of the photolysis beam) state-selectively ionizes the nascent D_2 via the Q-branch members of the $E,F\ ^1\Sigma_g^+$-$X\ ^1\Sigma_g^+$ band by [2+1] resonance-enhanced multiphoton ionization (REMPI).[15,16] The wavelength of the probe laser is scanned over the Doppler profile (~30 pm) of the REMPI line and the D_2^+ ions are accelerated toward a position-sensitive delay-line detector that records their three-dimensional velocity distribution using TOF voltages of $V_{acc}=-56.2$ V and $V_{ext}=-18.8$ V. These particular voltages are chosen so that our TOF operates under Wiley–McLaren space focusing conditions and the ion stream covers the maximum amount of area on our detector. It should be noted that owing to the similarity of the photolysis and REMPI wavelengths involved in this experiment, the probe laser can both photolyze the DBr bond and ionize the D_2 products within the duration of one laser pulse, producing a background signal. Therefore we alternate the delay time between the photolysis and probe laser pulses on an every-other-shot basis such that "one-laser" signal ions correspond to those that are produced when the probe laser pulse arrives before the photolysis laser pulse, and "two-laser" signal ions correspond to those that are produced when the probe laser pulse arrives ~10 ns after the photolysis laser pulse. Typically, data are acquired until 2000–10 000 ions (remaining after subtraction of one-laser background ions) have been collected. The ratio of the two-laser signal ions to the one-laser signal ions ranges from 1.3 to 2.0. Care is taken to ensure that all nascent D_2 products in a selected vibrational-rotational state are detected without bias, that is, without a correction for escaping the ionization volume.

III. RESULTS

For the D+DBr reaction there exist four possible channels

$$D(\text{fast}) + DBr \rightarrow D_2 + Br, \tag{1a}$$

$$D(\text{fast}) + DBr \rightarrow D_2 + Br^*, \tag{1b}$$

$$D(\text{slow}) + DBr \rightarrow D_2 + Br, \tag{1c}$$

$$D(\text{slow}) + DBr \rightarrow D_2 + Br^*. \tag{1d}$$

Channels (1b) and (1c) are energetically the same. Consequently, we should expect at most three channels to appear in

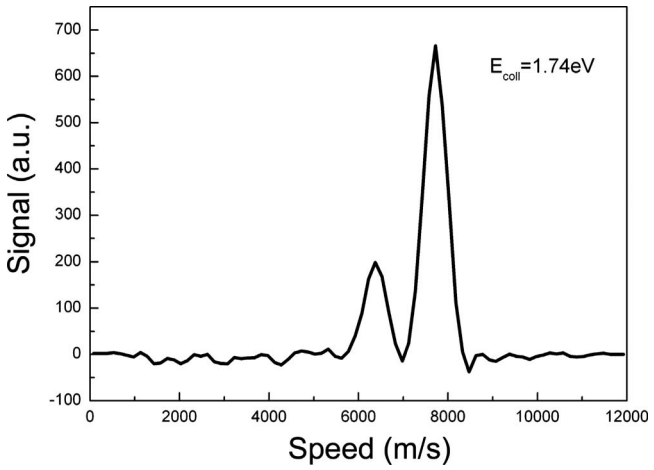

FIG. 2. Speed distribution of D_2 ($v'=2$, $J'=11$).

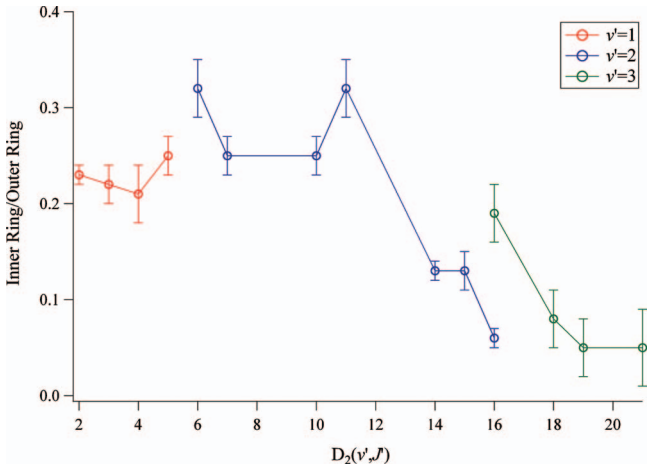

FIG. 3. $D_2(v',J')$ product population ratios from reaction channel (1c) (inner ring) divided by reaction channel (1a) (outer ring). Experiments measuring $D_2(v'=1,2,J')$ products were carried out at a collision energy of 1.74 eV, while those measuring $D_2(v'=3, J')$ products were at a collision energy of 1.84 eV. In both cases, the collision energy corresponds to that of channel (1a). The uncertainty represents one standard deviation from three repeated measurements.

our ion images. Figure 1 shows a typical three-dimensional crushed ion image [Fig. 1(a)] and the two-dimensional center slice [Fig. 1(b)] for the reaction yielding $D_2(v'=2, J'=11)$. It is evident at once from Fig. 1(b) that only two rings are observed. The outer ring appears at the energy of channel (1a). For all D_2 product states and collision energies no ring appears at the energy of channel (1d). Because channels (1b) and (1d) differ only in the collision energy of the D atom and the reaction cross section does not vary strongly with collision energy (*vide infra*), we conclude that the inner ring comes exclusively from channel (1c). Figure 2 shows the $D_2(v'=2, J'=11)$ speed distribution found from analyzing the images shown in Fig. 1. The fast peak dominates the slow peak and there is no evidence for a peak corresponding to reaction channel (1d). In addition, we are confident in assigning the rings in Fig. 1(b) or equivalently the peaks in Fig. 2 to a particular channel because the measured speed distributions closely match theoretical predictions. The $D_2(v'=2, J'=11)$ state, for example, has an allowed speed range for channel (1a) of 7562–8189 and 6239–6783 m/s for channel (1c). Inspection of Fig. 2 reveals a peak at 7786 m/s with a full width at half maximum (FWHM) of 510 m/s and another one at 6403 m/s with a FWHM of 523 m/s. A straightforward comparison of the calculated and experimentally measured values unambiguously determines the identity of peaks in Fig. 2. It should be also noted that the observed peak widths approach the resolution of our instrument,[13,17] which is about 500 m/s.

We studied this reaction system for numerous D_2 product states and for various collision energies. Figure 3 displays the population branching ratios in all cases except for the production of $D_2(v'=2, J'=12)$ and $D_2(v'=1, J'=20)$, which deserve special mention. In each case we found only two rings, which arise from reaction channels (1a) and (1c). Hence, we find no evidence for the nonadiabatic channels (1b) and (1d), within our experimental uncertainties. We estimate that any nonadiabatic contribution is less than 1% of the reaction process.

Examination of Fig. 3 reveals that the production of $D_2(v'=3, J')$ is generally about five times larger for fast D atoms than slow D atoms in the reaction of D+DBr. This ratio closely matches the production of fast D atoms compared with slow D atoms from the photolysis of DBr. Thus, we conclude that the reaction cross sections for these product states do not vary rapidly with collision energy. The same appears to be true for $D_2(v'=2$, low $J')$ but as we look at the production of $D_2(v'=2$, high $J')$ and $D_2(v'=1$, high $J')$ it seems clear that fast D atoms are more effective than slow D atoms in populating these product states. These findings can possibly be rationalized by understanding that fast D atoms for the same collision impact parameter introduce more angular momentum into the collision process than slow D atoms.

Figures 4(a) and 4(b) show the crushed three-dimensional ion image and two-dimensional slice for the simultaneous detection of $D_2(v'=2, J'=12)$ and $D_2(v'=1, J'=20)$. Initially, we thought that we were only observing the $D_2(v'=2, J'=12)$ product, so that the appearance of three rings was believed to be a clear signature for nonadiabatic behavior of a rather remarkable sort. Furthermore, it is seen from the speed distribution in Fig. 5 that the middle peak [channels (1b) and (1c)] has a greater intensity than the peak corresponding to channel (1a). This fact at first led us to think that we had found a case of a super nonadiabatic effect, which had not been observed previously. However, more investigation showed that the ion images presented in Figs. 4(a) and 4(b) come from a coincidence in which $D_2(v'=1, J'=20)$ is just 0.45 eV higher in energy than $D_2(v'=2, J'=12)$, an energy that is almost the same as the spin-orbit splitting of the bromine atom. Consequently, the calculated speed range for channel (1c) forming $D_2(v'=2, J'=12)$ is 5992–6536 m/s, while channel (1a) for $D_2(v'=1, J'=20)$ state has a predicted range of 5885–6512 m/s. Bearing in mind the resolution of our experimental apparatus, it is realized that the two channels cannot be resolved, as is evidenced by the middle peak in Fig. 5. In addition to the above coincidence, the REMPI lines for these two states differ in wavelength by less than 1 pm.

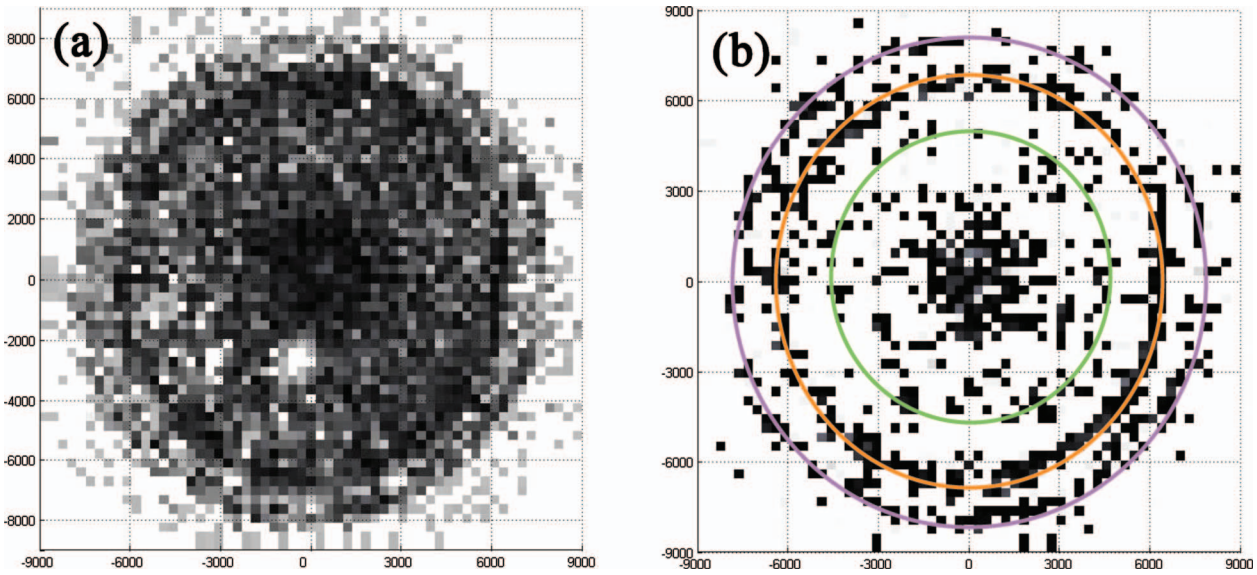

FIG. 4. Typical raw data for the simultaneous detection of both $D_2(v'=2,\ J'=12)$ and $D_2(v'=1,\ J'=20)$ showing (a) the three-dimensional crushed ion image and (b) the corresponding center slice. Three rings are visible from the sliced image. The innermost ring (green) corresponds to $D_2(v'=1,\ J'=20)$ products from channel (1c), the middle ring (orange) corresponds to both $D_2(v'=1,\ J'=20)$ products from channel (1a) and $D_2(v'=2,\ J'=12)$ products from channel (1c), and the outermost ring (purple) corresponds to $D_2(v'=2,\ J'=12)$ products from channel (1a).

We carried out a study of the simultaneous detection of these two products as a function of collision energy (Figs. 6 and 7). In order to decompose the middle peak in the speed distributions we make the assumption that the slow/fast channel branching ratios for $D_2(v'=2,\ J'=12)$ and $D_2(v'=2,\ J'=11)$ states are similar. For a given collision energy, inspection of contiguous D_2 states (see Fig. 3), e.g., $D_2(v'=2,\ J'=10)$ versus $D_2(v'=2,\ J'=11)$, $D_2(v'=2,\ J'=14)$ versus $D_2(v'=2,\ J'=15)$, and all $D_2(v'=1,\ J')$ states, reveals a minor variation of a few percent in most cases, except for the $D_2(v'=2,\ J'=10)$ versus $D_2(v'=2,\ J'=11)$ pair that exhibits ~20% difference. Hence, using the branching ratio for $D_2(v'=2,\ J'=11)$ at a collision energy of 1.74, 1.88, and 1.97 eV, we are able to separate the two contributions. The results are presented in Fig. 8. For clarity we add the intensities of the two channels (1a) and (1c) for the $D_2(v'=2,\ J'=11)$ state and for the $D_2(v'=1,\ J'=20)$ state. It is evident that with increasing collision energy formation of highly rotationally excited $D_2(v'=1,\ J'=20)$ increases whereas that of $D_2(v'=2,\ J'=12)$ decreases. Again, this can be explained by the fact that as the collision energy increases relatively more D atoms have enough angular momentum to form $D_2(v'=1,\ J'=20)$ compared with $D_2(v'=2,\ J'=12)$. It is clear from the above analysis that we detect both reaction products at the same time. With an understanding of this coincidence, we find again no evidence within our signal-to-noise ratio for the production of Br^* from D+DBr.

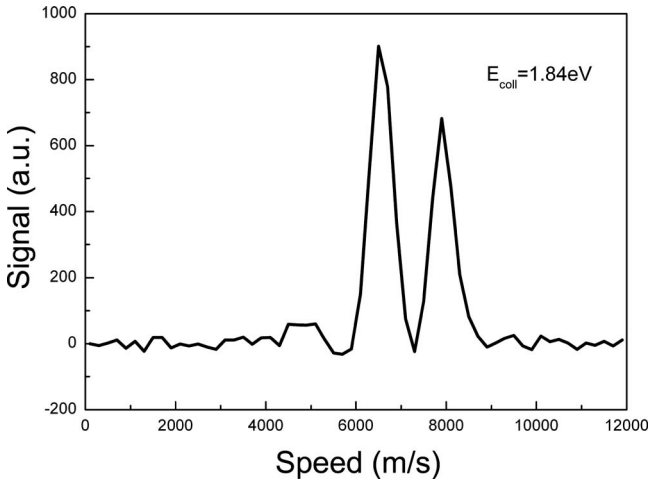

FIG. 5. Speed distribution from the simultaneous detection of both $D_2(v'=2,\ J'=12)$ and $D_2(v'=1,\ J'=20)$.

IV. DISCUSSION

Often it is thought that all the properties of a chemical reaction can be fully understood by knowing only the poten-

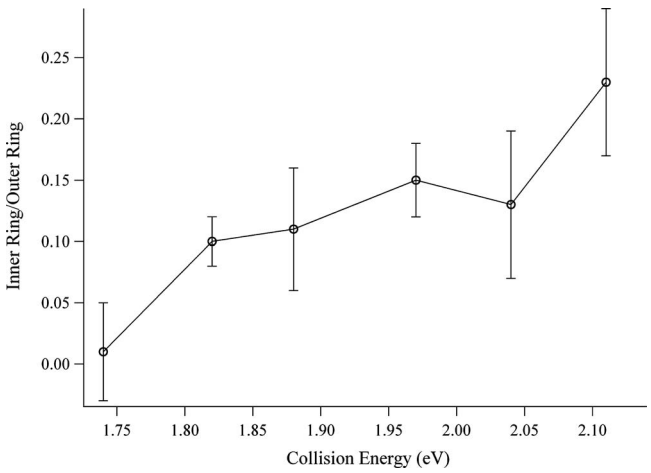

FIG. 6. Ratio of $D_2(v'=1,\ J'=20)$ product population from reaction channel (1c) (inner ring) to $D_2(v'=2,\ J'=12)$ product population from channel (1a) (outer ring) as a function of collision energy. The collision energy refers to that for channel (1a) for $D_2(v'=2,\ J'=12)$. The uncertainty represents one standard deviation from three repeated measurements.

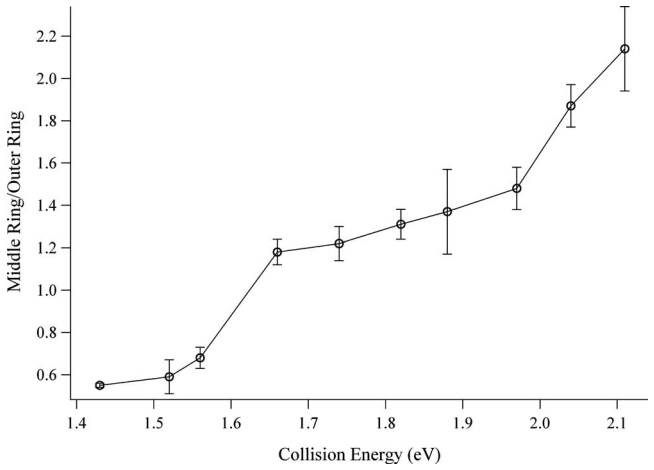

FIG. 7. Ratio of $D_2(v'=1,\ J'=20)$ product population from reaction channel (1a) and $D_2(v'=2,\ J'=12)$ from channel (1c) (middle ring) to $D_2(v'=2,\ J'=12)$ product population from channel (1a) (outer ring) as a function of collision energy The collision energy refers to that for channel (1a) for $D_2(v'=2,\ J'=12)$. The uncertainty represents one standard deviation from three repeated measurements.

tial energy surface that governs the motions of the nuclei. This notion is based on the Born–Oppenheimer approximation in which the motions of the light electrons readjust almost instantaneously to the positions of the heavy nuclei as the nuclei slowly move on a single potential energy surface. The validity of the Born–Oppenheimer approximation rests, in turn, on the large separation between the electronic states of a molecule compared with the separations between its vibrational and rotational levels. The Born–Oppenheimer approximation is expected to be particularly valid for reactions that take place with reactants in their ground electronic states. On the other hand, reactions involving excited-state reagents in which electronic states draw close or even cross are expected to lead to a breakdown of the Born–Oppenheimer approximation so that the nuclear motions no longer necessarily follow adiabatically the slowly changing potential energy surface but may undergo sudden nonadiabatic transitions in which a hop is made from one electronic

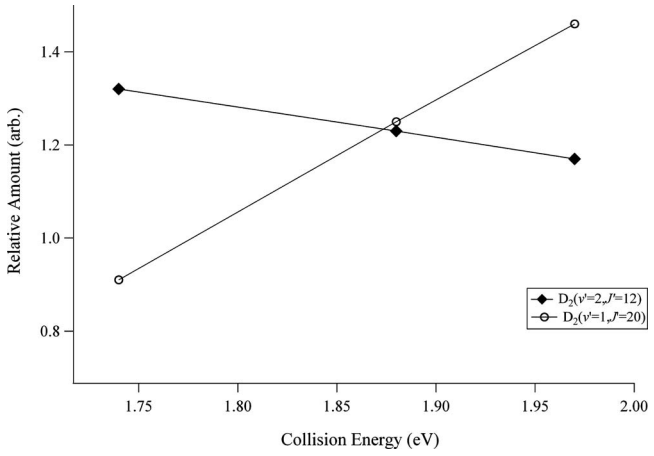

FIG. 8. Relative amounts of $D_2(v'=2,\ J'=12)$ and $D_2(v'=1,\ J'=20)$ product states, all normalized to the intensity of product $D_2(v'=2,\ J'=12)$ from channel (1a) as a function of collision energy. Each data point is a sum of channels (1a) and (1c) for one of the two D_2 rovibrational states. The collision energy refers to that for channel (1a) for $D_2(v'=2,\ J'=12)$.

state to another. Thus, in gas-phase ground-state chemical reactions, the Born–Oppenheimer approximation is the key starting point to understanding the dynamics, whereas in gas-phase photodissociation processes, nonadiabatic behavior often occurs.[18] Nonadiabatic processes are known to occur when molecules strike metal surfaces and they are also well established in various excited-state radiationless processes, but nonadiabatic behavior in elementary gas-phase reactions involving ground-state species seems to be exceptional.[19]

We have investigated the reaction of a fast ground-state deuterium atom (D) with a ground-state deuterium bromide (DBr) molecule under single-collision conditions using ion imaging. By examining various $D_2(v',J')$ vibrational-rotational product states, we find no detectable production of spin-orbit-excited Br atoms, $Br(^2P_{1/2})$, over a wide set of collision energies. This finding agrees with what is expected for a reaction proceeding along the minimum energy path in which the D atom approaches the DBr molecule in a straight line directed toward the D-end of the molecule (collinear collision geometry).

To make the significance of this last statement clearer, consider the reverse reaction of $Br+D_2$ to form DBr+D. Collinear approach is preferred, that is, the minimum energy path favors the linear geometry of the BrDD triatomic molecule. The approach of a Br atom in its $^2P_{3/2}$ ground spin-orbit state has a projection on the internuclear axis of the total electronic angular momentum of either $\Omega=1/2$ or $\Omega=3/2$. The $\Omega=1/2$ electronic state correlates with $D(^2S_{1/2})+DBr(^1\Sigma^+_0)$, and the $\Omega=3/2$ electronic state correlates with $D(^2S_{1/2})+DBr(^3\Pi_{1,2})$. Because the electronically excited $DBr(^3\Pi)$ triplet state lies so high above the $DBr(^1\Sigma^+_0)$ ground state, the $\Omega=3/2$ potential energy surface does not lead to product formation. Consider as well the approach of a Br atom in its $^2P_{1/2}$ excited spin-orbit state to $D_2(^1\Sigma^+_0)$. This collision process leads to another $\Omega=1/2$ potential energy surface which lies above the ground $\Omega=1/2$ state and correlates once again with $D(^2S_{1/2})+DBr(^3\Pi_{0,1})$. Thus, it is expected on simple theoretical grounds that spin-orbit-excited bromine atoms make a negligible contribution to the reaction of Br with D_2. The same reasoning applies to $Cl+H_2$ (Refs. 20 and 21) and $F+H_2$ (Refs. 1 and 22–31) for which almost all the experimental evidence and theoretical calculations support the conclusion that spin-orbit-excited halogen atoms are almost totally unreactive in collisions with molecular hydrogen.

At first, it might be wondered if deviations from collinearity remove the nonadiabatic nature of the $D_2+Br^* \leftrightarrow D+DBr$ reaction. Dagdigian and Campbell[32] have presented a general argument why only Br and not Br^* should be expected to take part in this reaction. Consider the interaction of a bromine atom with a hydrogen molecule in arbitrary bent (C_S) geometry. The surface corresponding to the p orbital hole in the triatomic plane ($1\ ^2A'$) leads to reaction, whereas the two out-of-plane p-hole orientations result in repulsive interactions and connect to energetically inaccessible electronically excited products. When spin-orbit interaction is included, the doubly degenerate $Br(^2P_{1/2})$ state correlates with the $2\ ^2A'$ surface, whereas the fourfold degenerate lower $Br(^2P_{3/2})$ state correlates with the reactive

$1\,^2A'$ and unreactive $^2A''$ surfaces. Much work has been done calculating the nature of the potential energy surfaces of the BrHH system and the findings are consistent with the above argument.[33–37]

In comparison, the experimental and theoretical work on H+HBr reaction is much sparser. In 1981, Polanyi and co-workers[12] examined the H+HBr reaction using different isotopes of hydrogen. They found a substantial isotope effect on the ground-state reaction but did not investigate Br^* production. In 1989, Valentini and co-workers[10,35] carried out experimental studies of H+HBr at a collision energy of 1.6 eV and obtained the product rotational distributions both for the abstraction reaction and for the combined inelastic collisions and exchange reactions. They interpreted their results to be a consequence of a highly favored collinear approach geometry. This conclusion was challenged later by Pomerantz *et al.*[11] who observed a small fraction of product $H_2(v'=2, J')$ molecules produced in rotational levels so high that their production cannot be consistent with a near collinear approach. With the help of quasiclassical trajectory calculations, they interpreted the formation of these high rotational levels to result from hydrogen-atom roaming, which proceeds from a bent transition state. Further support for this migratory reaction model has been provided by the theoretical study of Fu *et al.*[38] who used a time-dependent wave packet method to calculate differential cross sections on the Kurosaki–Takayanagi[39] potential energy surface. There have been further improvements on the HHBr potential energy surface,[40–43] but unfortunately, these studies do not provide us with much information about the possible production of Br^*. There seems to be a consensus, however, that the electronically nonadiabatic transitions from $Br(^2P_{1/2})+H_2(v)$ to $Br(^2P_{3/2})+H_2(v+1)$ effectively occur in the entrance region of the potential surface but the contribution of the electronically nonadiabatic chemical reaction, $Br(^2P_{1/2})+H_2(v) \rightarrow HBr+H$, is small.

The only evidence for the formation of significant amounts of Br^* from the H+HBr reaction comes from the H_2/Br_2 low-pressure flow study of Nesbitt and Leone.[9] They used 473 nm radiation to photolyze Br_2. This wavelength was chosen because it produces a significant amount of Br^* with a quantum yield[44] of about 0.7. Br^* is efficiently quenched by $H_2(v=0)$ to produce $Br+H_2(v=1)$ in a nearly resonant energy transfer process. Nesbitt and Leone observed infrared chemiluminescence at about 3.85 μm from vibrationally excited HBr. This observation was interpreted to arise from the reaction of Br^* with $H_2(v=1)$ to produce HBr+H followed by the reaction $H+Br_2(\text{excess}) \rightarrow HBr(v' \leq 5)+Br$. They reach the conclusion that spin-orbit-excited $Br(^2P_{1/2})$ atoms react efficiently with $H_2(v=1)$ to produce $HBr(v'=0)+H(\text{fast})$. They speculate that the presence of near resonant electronic to vibrational transfer in the entrance channel, namely, the transformation of the $[Br^*+H_2(v'=1)]$ collision complex to the $[Br+H_2(v'=2)]$ collision complex, facilitates redirecting the energy into the reaction coordinate for forming $HBr(v'=0)+H$. At first, it seemed to us difficult to reconcile the observations of Nesbitt and Leone with those of this work. After careful reflection, however, we have come to the realization that it is not possible to compare rigorously these two experiments as they have been carried out under quite different conditions. Not only is there the problem of what substituting D for H does to the process but also there is the problem that these two experiments are not the time reversal of one another.

Clearly, yet more experiments are needed along with a calculation of the cross sections for the adiabatic and nonadiabatic channels on the chemically reliable potential energy surfaces to understand more completely to what extent does the nonadiabatic reaction of hydrogen with hydrogen bromide occur to produce molecular hydrogen and spin-orbit-excited bromine. We do know from this work that for the collision energies and internal states that we studied, the nonadiabatic channel is of negligible importance.

ACKNOWLEDGMENTS

We are grateful to D. J. Nesbitt for useful discussions. This work was supported by the National Science Foundation under Grant No. NSF CHE-0650414.

[1] D. M. Neumark, A. M. Wodtke, G. N. Robinson, C. C. Hayden, and Y. T. Lee, J. Chem. Phys. **82**, 3045 (1985).
[2] W. W. Harper, S. A. Nizkorodov, and D. J. Nesbitt, J. Chem. Phys. **116**, 5622 (2002).
[3] L. Che, Z. Ren, X. Wang, W. Dong, D. Dai, X. Wang, D. H. Zhang, X. Yang, L. Sheng, G. Li, H.-J. Werner, F. Lique, and M. H. Alexander, Science **317**, 1061 (2007).
[4] S. H. Lee, L.-H. Lai, K. Liu, and H. Chang, J. Chem. Phys. **110**, 8229 (1999).
[5] F. Dong, S.-H. Lee, and K. Liu, J. Chem. Phys. **115**, 1197 (2001).
[6] N. Balucani, D. Skouteris, L. Cartechini, G. Capozza, E. Segoloni, P. Casavecchia, M. H. Alexander, G. Capecchi, and H.-J. Werner, Phys. Rev. Lett. **91**, 013201 (2003).
[7] E. Garand, J. Zhou, D. E. Manolopoulos, M. H. Alexander, and D. M. Neumark, Science **319**, 72 (2008).
[8] X. Wang, W. Dong, C. Xiao, L. Che, Z. Ren, D. Dai, X. Wang, P. Casavecchia, X. Yang, B. Jiang, D. Xie, Z. Sun, S.-Y. Lee, D. H. Zhang, H.-J. Werner, and M. H. Alexander, Science **322**, 573 (2008).
[9] J. Nesbitt and S. R. Leone, J. Chem. Phys. **73**, 6182 (1980).
[10] P. M. Aker, G. J. Germann, and J. J. Valentini, J. Chem. Phys. **90**, 4795 (1989).
[11] A. E. Pomerantz, J. P. Camden, A. S. Chiou, F. Ausfelder, N. Chawla, W. L. Hase, and R. N. Zare, J. Am. Chem. Soc. **127**, 16368 (2005).
[12] J. W. Hepburn, D. Klimek, K. Liu, R. G. Macdonald, H. R. Mayne, F. J. Northrup, and J. C. Polanyi, Int. J. Chem. Kinet. **13**, 845 (1981).
[13] K. Koszinowski, N. T. Goldberg, A. E. Pomerantz, and R. N. Zare, J. Chem. Phys. **125**, 133503 (2006).
[14] K. Koszinowski, N. T. Goldberg, J. Zhang, R. N. Zare, F. Bouakline, and S. C. Althorpe, J. Chem. Phys. **127**, 124315 (2007).
[15] A. J. Heck, W. M. Huo, R. N. Zare, and D. W. Chandler, J. Mol. Spectrosc. **173**, 452 (1995).
[16] A. E. Pomerantz, F. Ausfelder, R. N. Zare, and W. M. Huo, Can. J. Chem. **82**, 723 (2004).
[17] N. T. Goldberg, K. Koszinowski, A. E. Pomerantz, and R. N. Zare, Chem. Phys. Lett. **433**, 439 (2007).
[18] D. C. Clary, Proc. Natl. Acad. Sci. U.S.A. **105**, 12649 (2008).
[19] A. M. Wodtke, J. C. Tully, and D. J. Auerbach, Int. Rev. Phys. Chem. **23**, 513 (2004).
[20] D. Skouteris and D. E. Manolopoulos, Science **286**, 1713 (1999).
[21] S. H. Lee and K. P. Liu, J. Chem. Phys. **111**, 6253 (1999).
[22] D. M. Neumark, A. M. Wodtke, G. N. Robinson, C. C. Hayden, and Y. T. Lee, Phys. Rev. Lett. **53**, 226 (1984).
[23] K. Stark and H.-J. Werner, J. Chem. Phys. **104**, 6515 (1996).
[24] J. F. Castillo, D. E. Manolopoulos, K. Stark, and H.-J. Werner, J. Chem. Phys. **104**, 6531 (1996).
[25] J. F. Castillo, B. Hartke, H.-J. Werner, F. J. Aoiz, L. Bañares, and B. Martinez-Haya, J. Chem. Phys. **109**, 7224 (1998).
[26] M. Qiu, Z. Ren, L. Che, D. Dai, S. A. Harich, X. Wang, X. Yang, C. Xu, D. Xie, M. Gustafsson, R. T. Skodje, Z. Sun, and D. H. Zhang, Science

311, 1440 (2006).
[27] M. H. Alexander, D. E. Manolopoulos, and H.-J. Werner, J. Chem. Phys. **113**, 11084 (2000).
[28] M. Faubel, L. Rusin, S. Schlemmer, F. Sondermann, U. Tappe, and J. P. Toennies, J. Chem. Phys. **101**, 2106 (1994).
[29] M. Faubel, B. Martınez-Haya, L. Y. Rusin, U. Tappe, and J. P. Toennies, J. Phys. Chem. A **101**, 6415 (1997).
[30] F. Rebentrost and W. A. Lester, Jr., J. Chem. Phys. **67**, 3367 (1977).
[31] J. C. Tully, J. Chem. Phys. **60**, 3042 (1974).
[32] P. J. Dagdigian and M. L. Campbell, Chem. Rev. (Washington, D.C.) **87**, 1 (1987).
[33] T. Takayanagi and Y. Kurosaki, J. Chem. Phys. **113**, 7158 (2000).
[34] Y. L. Volobuev, M. D. Hack, and D. G. Truhlar, J. Phys. Chem. A **103**, 6225 (1999).
[35] P. M. Aker, G. J. Germann, K. D. Tabor, and J. J. Valentini, J. Chem. Phys. **90**, 4809 (1989).
[36] S. L. Mielke, G. J. Tawa, D. G. Truhlar, and S. W. Schwenke, Chem. Phys. Lett. **234**, 57 (1995).
[37] S. L. Mielke, D. G. Truhlar, and S. W. Schwenke, J. Phys. Chem. **99**, 16210 (1995).
[38] B. Fu, Y. Zhou, and D. H. Zhang, J. Theor. Comput. Chem. **7**, 777 (2008).
[39] Y. Kurosaki and T. Takayanagi, J. Chem. Phys. **119**, 7838 (2003).
[40] Y. Kurosaki and T. Takayanagi, Chem. Phys. Lett. **406**, 121 (2005).
[41] W.-L. Quan, Q. Song, and B.-Y. Tang, Chem. Phys. Lett. **437**, 165 (2007).
[42] J. Kłos, M. M. Szczesniak, and G. Chalasinski, J. Phys. Chem. A **106**, 7362 (2002).
[43] J. Klos, M. M. Szczesniak, and G. Chalasinski, Int. Rev. Phys. Chem. **23**, 541 (2004).
[44] H. K. Haugen, E. Weitz, and S. R. Leone, J. Chem. Phys. **83**, 3402 (1985).